HHS Public Access

Author manuscript

*Nat Nanotechnol*. Author manuscript; available in PMC 2011 February 01.

Published in final edited form as:

*Nat Nanotechnol*. 2010 August ; 5(8): 607–611. doi:10.1038/nnano.2010.126.

# Delivery of molecules into cells using carbon nanoparticles activated by femtosecond laser pulses

**Prerona Chakravarty**,

Ph.D. Graduate, School of Chemical & Biomolecular Engineering, Georgia Institute of Technology, 311 Ferst Drive, Atlanta, GA 30332, prerona@gmail.com

**Wei Qian**,

Senior Research Scientist and Assistant Director of the Laser Dynamics Laboratory, School of Chemistry and Biochemistry, Georgia Institute of Technology, Laser Dynamics Laboratory, School of Chemistry and Biochemistry, Georgia Institute of Technology, Atlanta, GA 30332, wei.qian@chemistry.gatech.edu

**Mostafa A. El-Sayed**, and

Julius Brown Chair and Regents Professor; Director of the Laser Dynamics Laboratory, School of Chemistry and Biochemistry, Georgia Institute of Technology, Laser Dynamics Laboratory, School of Chemistry and Biochemistry, Georgia Institute of Technology, Atlanta, GA 30332 mostafa.el-sayed@chemistry.gatech.edu

**Mark R. Prausnitz**

Professor, School of Chemical & Biomolecular Engineering, Georgia Institute of Technology, 311 Ferst Drive, Atlanta, GA 30332, prausnitz@gatech.edu, Phone: 404-894-5135, Fax: 404-894-2291

## Abstract

A major barrier to drug and gene delivery is crossing the cell's plasma membrane. Physical forces applied to cells via electroporation1, ultrasound2 and laser-irradiation3–6 generate nanoscale holes in the plasma membrane for direct delivery of drugs into the cytoplasm. Inspired by previous work showing that laser excitation of carbon nanoparticles can drive the carbon-steam reaction to generate highly controlled shock waves7–10, here we show carbon black (CB) nanoparticles activated by femtosecond laser pulses can facilitate the delivery of small molecules, proteins and DNA into two types of cells. Our initial results suggest that interaction between the laser energy and CB nanoparticles may generate photoacoustic forces by chemical reaction to create transient holes in the membrane for delivery.

This study was motivated by the need for more efficient intracellular delivery of agents such as DNA vaccines11, short-interfering RNA12, lysosomal enzymes13 and anticancer



Correspondence and requests for materials should be addressed to M.R.P..

Supplementary information accompanies this paper at www.nature.com/naturenanotechnology.

chemotherapeutics14. Existing biological delivery methods such as viral vectors can be efficient but are often accompanied by side effects like mutagenicity and host-immune rejection15. Chemical formulations such as cationic lipids and polymers have drawbacks associated with endocytic degradation, targeting inefficiency and the need for cell type-specific formulations16. Physical methods using electroporation, ultrasound and laser irradiation generally avoid difficulties associated with active transport mechanisms of the cells and can apply to many cell types, but are often inefficient17.

Here we used CB nanoparticles activated by ultrashort laser pulses to create transient openings in the cell plasma membrane. Previously, laser- and ultrasound- mediated cavitation experiments showed that transient bubble collapse can permeabilize the cell membrane and allow uptake of molecules, but typically with extensive loss of cell viability2, 18–21. We show here that laser-activation of CB can drive small molecules, proteins and DNA into different types of cells with high efficiency, while maintaining high cell viability.

To determine whether laser-activation of CB can facilitate efficient intracellular uptake in viable cells, we exposed suspensions of human prostate-cancer cells and CB nanoparticles in the presence of calcein, bovine serum albumin (BSA), or plasmid DNA encoding luciferase expression to 800nm femtosecond laser pulses at intensities previously shown to initiate photoacoustic activity10. While cells exposed to laser alone or CB alone showed little uptake (see below), confocal microscopy showed intracellular uptake of all three compounds, indicating that laser irradiation of CB permeabilized cells. Calcein uptake was visualized across many cells (Figure 1a) and found throughout the cytosol and nucleus (Figure 1b). BSA was mostly in cytosol but not the nucleus since BSA is larger than nuclear pores (Figure 1c). DNA appeared uneven and highly localized at some points probably due in part to slow diffusion in cytosol (Figure 1d)22. This analysis is consistent with cell permeability increases that selectively breach the plasma membrane.

Quantitative flow cytometry in Figure 2 shows that, relative to non-irradiated exposures, >90% of DU145 prostate cancer cells were calcein-positive and more than 35% were BSA-positive (Figure 2a). In non-irradiated controls, cells were not irradiated, but subjected to all other procedures. Average number of molecules delivered to treated cells was on the order of $10^6$ calcein molecules/cell and $10^5$ BSA molecules/cell (Figure 2c). The resulting intracellular molecule concentrations were 2.0±0.1μM for calcein and 0.9±0.1μM for BSA, which are approximately one order of magnitude less than the extracellular concentration of 10μM. Cell viability remained close to 100% (Figure 2b).

Similar results were also seen in a GS-9L gliosarcoma cell line, although uptake (Figure 2a) and viability (Figure 2b) were somewhat lower. In additional experiments with the prostate cancer cells, up to 22% of cells exhibited intracellular uptake of fluorescently labeled DNA (black bars in Figure 3) and expression of luciferase was increased 17-fold in treated cells over non-irradiated samples (grey bars in Figure 3). This shows that DNA was not only delivered into cells, but was in a functional form capable of transfecting cells to drive protein expression (see S.I. Section 2 for further discussion). Altogether, these results demonstrate that laser-activated CB can efficiently deliver a range of different molecules into multiple cell types.

Concerning operating parameters, Figure 4a shows that intracellular uptake of calcein increased with laser fluence and exposure time. At fluences of 2-5mJ/cm$^2$, there was uptake by up to 40% of cells with no significant loss in cell viability (Figure 4b). At a fluence of 10mJ/cm$^2$, uptake increased, went through a maximum of 80% at 3min, and then decreased to 1% after 20min. ANOVA analysis showed that fluence and exposure time both significantly impacted uptake. Viability was not significantly affected for fluence <5mJ/cm$^2$ and exposure time <10min, but was decreased by more than 70% at the most intense conditions studied (Figure 4b). Uptake also increased with CB concentration while viability remained unchanged (Figure S1 in S.I.).

These data indicate that intracellular uptake of molecules requires a synergistic interaction between laser irradiation and CB. As shown in Figure 5, laser irradiation at specified conditions delivered calcein molecules into almost 70% of cells (condition A). In contrast, (i) mixing cells with CB at the same conditions, but in the absence of laser exposure resulted in no uptake (condition B) and (ii) applying laser energy at the same conditions, but without CB, also yielded almost no uptake (<2% cells, condition C). Because neither laser irradiation alone nor CB alone had significant cellular effects, a synergistic interaction between laser irradiation and CB is needed for intracellular uptake.

Our data further show that the specific properties of CB are critical to generating intracellular uptake. While we found that laser-irradiation with CB drives extensive intracellular uptake, identical irradiation with multiwalled carbon nanotubes (MWNT, Figure 2) or gold nanorods (Figure 5, condition D) had little or no significant effect, respectively. CB, MWNT and gold nanoparticles all absorb laser energy and reach very high surface temperatures upon laser irradiation23, 24. Moreover, MWNT and gold nanorods were added at concentrations adjusted to absorb the same energy as CB, thereby releasing the same amount of heat and possibly emitting stable acoustic waves7, 25. This suggests that thermal effects, such as water vaporization or explosive particle disintegration, are not directly responsible for intracellular delivery.

In contrast, we note that CB has a much more chemically reactive surface compared to MWNT and gold nanorods26, 27. Previous studies showed carbon-steam reaction, $C(s)+H_2O(l)\rightarrow CO(g)+H_2(g)$, during laser irradiation of CB at conditions similar to those used in this study7–10. Because carbon in CB nanoparticles is a reactant that is consumed during the carbon-steam reaction, we monitored the consumption of carbon in our experiments by measuring laser light transmittance through the CB suspension. We found that transmittance of the incident laser light increased over time during irradiation, which suggests a decrease in CB nanoparticle size and concentration probably due to consumption of carbon (Figure S2 in S.I.). Thus, chemical reaction of CB may explain the specific need for CB to enable intracellular uptake in this study.

Previous studies also showed that rapid generation of gas by carbon-steam reaction under conditions similar to those used in this study produced cavitational shockwaves as a photoacoustic effect7–10. Shockwaves generated by other methods have separately been shown to permeabilize cells to enable intracellular uptake2–6. We therefore hypothesized that photoacoustic activity generated by the carbon-steam reaction during laser irradiation of

CB seen in other studies may similarly occur in this study and, further, may be responsible for intracellular uptake.

To assess this, we measured pressure in an exposure chamber containing CB as a function of laser fluence. Because the pressure transducer was not fast enough to capture pressure transients during each femtosecond pulse, we measured a time-averaged pressure, which should be much lower than the peak pressures achieved during transient bubble collapse. We found that pressure generated in the exposure chamber was elevated during laser irradiation and increased as a function of laser fluence (Figure S3 in S.I.), which is consistent with formation of gaseous reaction products, but could also be due to thermal or other effects.

We also found that a five-fold increase in viscosity lowered uptake to levels indistinguishable from the non-irradiated control (Figure 5, condition F). Although this five-fold increase in viscosity could also reduce calcein diffusivity by five fold, this reduced diffusion does not explain the complete suppression of uptake. Instead, acoustically driven bubble formation and shockwave propagation may have been dampened below the threshold for cell permeabilization. Further studies directly measuring acoustic bubble activity are needed to confirm this hypothesis.

An alternative explanation is that chemical products of the reaction directly affect cells without involvement of photoacoustic effects. To test this idea, we irradiated cell-free suspensions containing CB and calcein and then added cells within 1s after irradiation. Relative to the non-irradiated control (Figure 5, condition B), uptake was unchanged (Figure 5, condition E), suggesting that long-lived end products of chemical reaction were not responsible for uptake.

Finally, we assessed the possible role of endocytosis in intracellular uptake. We found that suppression of clathirin-mediated endocytosis by depleting intracellular $K^+$ had no significant effect on uptake (Figure 5, condition G), indicating that endocytosis by this mechanism was not involved. To determine the timescale of uptake, cells were irradiated with CB for 3min, after which calcein was added at different times after irradiation. Within 1s after irradiation, uptake efficiency decreased 12-fold and remained low at later times (Figure 5, conditions H1 – H4). This shows that increased cell permeability was short-lived and at least largely reversible.

Overall, our results show that laser-activated CB nanoparticles can be used to deliver small molecules, proteins and DNA efficiently into two types of cells while maintaining high cell viability. At optimized conditions, calcein uptake was seen in up to 90% of cells with ≥90% viability. Our results interpreted in the context of previous studies7–10 indicate that uptake occurs due to a specific interaction between laser energy and CB that may generate photoacoustic forces via laser-induced carbon-steam reaction to cause transient permeabilization of the cell membrane. This novel use of nanotechnology with advanced laser technology could provide an alternative to viral and chemical-based drug and gene delivery.

## Methods

### Cell sample preparation

Human prostate cancer cells (DU145, American Type Culture Collection, Manassas, VA) and rat gliosarcoma cells (GS-9L, courtesy of Henry Brem, Johns Hopkins University, Baltimore, MD) were cultured as described in S.I Section 1.1.

CB suspensions were prepared by sonicating aqueous solutions of carbon black (Black Pearls 470, Cabot, Billerica, MA) at 0.4mg/ml for ≥2min in presence of 0.1%(w/v) sodium-dodecyl-sulfate (Sigma-Aldrich, St. Louis, MO) to minimize particle aggregation. Individual CB nanoparticles had 25nm average diameter, but were mostly in aggregated form with 200nm average diameter (see S.I. Section 1.2) These were the same particles shown to cause laser-induced photoacoustic emissions in previous studies8, 10. In some experiments, CB were replaced with MWNT (NanoLab, Newton, MA), which had 30±15nm outer diameter and 1–5μm length or with gold nanorods with aspect ratio of 3.9 (See S.I. Section 1.2)28.

To measure intracellular uptake, solutions of fluorescent marker compounds dissolved in phosphate-buffered saline (PBS, Cellgro) were added to cell-CB suspensions before irradiation at a final concentration of 10μM calcein or FITC-labeled bovine serum albumin (BSA) (Molecular Probes, Eugene, OR). To measure intracellular DNA uptake, plasmid-DNA (6.7kbp or 4.4MDa, gWiz Luciferase, Adevron, Fargo, ND) was labeled by incubation with YOYO-1 dye (Molecular Probes) for 10min at a ratio of one YOYO-1 molecule per 10bp of plasmid DNA29 and then added to cell-CB suspensions at a final concentration of 4nM within 1s before irradiation. Fluorescence from marker compounds retained within cells was measured by flow cytometry after rinsing the cells, as described below.

To identify nonviable cells after irradiation, and eliminate them from analysis, propidium iodide (Molecular Probes), which stains nonviable cells with red fluorescence, was added to samples at a final concentration of 0.37μM at least 15min after irradiation and before assaying by flow cytometry30. DNA transfection was studied using the Luciferase Assay System (Promega, Madison, WI) 48h after irradiation, as described in S.I. Section 1.5.

To study effect of viscosity, the kinematic viscosity of the suspension medium was increased from 1.1cSt to 5.3cSt by adding carboxymethylcellulose (Sigma-Aldrich) to PBS at 400mg/ml. Viscosities were measured using a Cannon-Ubbelohde viscometer (50-B680, Cannon Instrument, State College, PA). Cells were pelleted and re-suspended in the more viscous media before irradiation.

To deplete cells of $K^+$, cells were centrifuged and pelleted in $K^+$-free buffer (140mM NaCl, 1mM $CaCl_2$, 1mM $MgCl_2$, 1mg/mL D-glucose in DI $H_2O$, pH 7.4) followed by hypotonic shock for 5 min in $K^+$-free buffer diluted 1:1 with DI water31. After 5 min, cells were spun down and re-suspended in full strength $K^+$-free buffer where they remained for the remainder of the experiment.

### Irradiation of cells

Cell samples were irradiated using a femtosecond Ti:Sapphire laser system (CPA-1000, Clark-MXr, Dexter, MI) as described previously24 and in S.I. Section 1.3. Exposure chambers were constructed from glass cylindrical cells (37-PX-2, Starna Cells, Atascadero, CA). The stem of the cell was cut to approximately 5mm, and fitted with a glass stopper. Samples were prepared by mixing known volumes of CB and uptake marker with 500μl of cell suspension and then aliquoting this solution into the exposure chamber, whose volume was approximately 560μl. The resulting small headspace filled with air facilitated mixing of the chamber contents during irradiation.

The chamber was then mounted on a custom-made stand that could three-dimensionally microposition the sample to obtain desired spot diameters of the incident laser beam. The contents of the chamber were mixed during irradiation in part by rotating the chamber at 5rpm manually. After irradiation, samples were transferred into 1.5ml microcentrifuge tubes and kept at room temperature for 5min. The tubes were then placed on ice until all samples had been irradiated (2–3h). Non-irradiated negative control samples were not irradiated, but subjected to all other procedures.

Unless otherwise specified, cell samples exposed to laser in presence of CB are referred to as “treated” and control cell samples not exposed to laser but subjected to all other treatments are referred to as “non-irradiated”.

### Cellular data acquisition and analysis

Flow cytometry (BD LSR, BD Biosciences, San Jose, CA) was used to determine molecular uptake, i.e., fraction of cells containing intracellular fluorescent molecules, number of fluorescent molecules per cell, and loss of cell viability by detecting the fluorescence intensity from uptake molecules and propidium iodide, respectively, on a cell-by-cell basis, as described previously30. A minimum of three replicates was performed for all conditions and the equality of mean responses was tested using analysis of variance (ANOVA, $\alpha$=0.05) using MINITAB (Minitab, State College, PA). Cells were also imaged using a Zeiss LSM 510 confocal laser-scanning microscope or Zeiss LSM META/NLO 510 multiphoton microscope (Zeiss, Thornwood, NY). See S.I. Section 1.5 for more information.

### Additional methods

More information can be found in S.I. on pressure measurements during irradiation (Section 1.4), and statistical methods (Section 1.6)

## Supplementary Material

Refer to Web version on PubMed Central for supplementary material.

## Acknowledgements

The authors thank Samuel Graham for use of his pressure measurement apparatus; Sankar Nair for technical discussions; and Jung-Hwan Park, Daniel Hallow, Robyn Schlicher, Joshua Hutcheson and Ying Liu for helpful discussions and laboratory assistance. This work was supported in part by the U.S. National Institutes of Health and

Institute of Paper Science and Technology and was carried out in the Institute for Bioengineering and Biosciences, Center for Drug Design, Development and Delivery, and Laser Dynamics Laboratory at Georgia Tech.

P.C. carried out the study in collaboration with W.Q., who provided laser expertise. M.R.P. and M.A.E. were the principal investigators. All authors participated in study design and interpretation. P.C. and M.R.P. wrote the paper.

## References

1. Bodles-Brakhop AM, Heller R, Draghia-Akli R. Electroporation for the delivery of DNA-based vaccines and immunotherapeutics: current clinical developments. Mol Ther. 2009; 17:585–592. [PubMed: 19223870]
2. Mitragotri S. Healing sound: the use of ultrasound in drug delivery and other therapeutic applications. Nat Rev Drug Discov. 2005; 4:255–260. [PubMed: 15738980]
3. Tao W, Wilkinson J, Stanbridge EJ, Berns MW. Direct gene transfer into human cultured cells facilitated by laser micropuncture of the cell membrane. Proc Natl Acad Sci U S A. 1987; 84:4180–4184. [PubMed: 3473500]
4. Tirlapur UK, Konig K. Targeted transfection by femtosecond laser. Nature. 2002; 418:290–291. [PubMed: 12124612]
5. Kodama T, Doukas AG, Hamblin MR. Shock wave-mediated molecular delivery into cells. Biochim Biophys Acta. 2002; 1542:186–194. [PubMed: 11853891]
6. Esenaliev RO, Larina IV, Larin KV, Motamedi M, Evers BM. Mechanism of laser-induced drug delivery in tumors. Proc. SPIE. 2000; 3914:188–196.
7. Löwen H, Madden PA. A microscopic mechanism for shock-wave generation in pulsed-laser-heated colloidal suspensions. J. Chem. Phys. 1992; 97:8760–8766.
8. Chen H, Diebold G. Chemical generation of acoustic waves: a giant photoacoustic effect. Science. 1995; 270:963–966.
9. Chen H, McGrath T, Diebold GJ. Laser chemistry in suspensions: new products and unique reaction conditions for the carbon-steam reaction. Angewandte Chemie International Edition in English. 1997; 36:163–166.
10. McGrath TE, Diebold GJ, Bartels DM, Crowell RA. Laser-initiated chemical reactions in carbon suspensions. J. Phys. Chem. A. 2002; 106:10072–10078.
11. Lu S, Wang S, Grimes-Serrano JM. Current progress of DNA vaccine studies in humans. Expert Rev Vaccines. 2008; 7:175–191. [PubMed: 18324888]
12. Whitehead KA, Langer R, Anderson DG. Knocking down barriers: advances in siRNA delivery. Nat Rev Drug Discov. 2009; 8:129–138. [PubMed: 19180106]
13. Desnick RJ. Enzyme replacement and enhancement therapies for lysosomal diseases. J Inherit Metab Dis. 2004; 27:385–410. [PubMed: 15190196]
14. Nobili S, Landini I, Giglioni B, Mini E. Pharmacological strategies for overcoming multidrug resistance. Curr Drug Targets. 2006; 7:861–879. [PubMed: 16842217]
15. Young LS, Searle PF, Onion D, Mautner V. Viral gene therapy strategies: from basic science to clinical application. J Pathol. 2006; 208:299–318. [PubMed: 16362990]
16. Lavigne MD, Gorecki DC. Emerging vectors and targeting methods for nonviral gene therapy. Expert Opin Emerg Drugs. 2006; 11:541–557. [PubMed: 16939390]
17. Mehier-Humbert S, Guy RH. Physical methods for gene transfer: improving the kinetics of gene delivery into cells. Adv Drug Deliv Rev. 2005; 57:733–753. [PubMed: 15757758]
18. Esenaliev RO. Application of light and ultrasound for medical diagnostics and treatment. Proc. SPIE. 2002; 4707:158–164.
19. ter Haar G. Therapeutic applications of ultrasound. Prog Biophys Mol Biol. 2007; 93:111–129. [PubMed: 16930682]
20. Hernot S, Klibanov AL. Microbubbles in ultrasound-triggered drug and gene delivery. Adv Drug Deliv Rev. 2008; 60:1153–1166. [PubMed: 18486268]
21. Hynynen K. Ultrasound for drug and gene delivery to the brain. Adv Drug Deliv Rev. 2008; 60:1209–1217. [PubMed: 18486271]

22. Lukacs GL, et al. Size-dependent DNA mobility in cytoplasm and nucleus. J Biol Chem. 2000; 275:1625–1629. [PubMed: 10636854]
23. Sun X, et al. Investigation of an optical limiting mechanism in multiwalled carbon manotubes. Appl. Opt. 2000; 39:1998–2001. [PubMed: 18345099]
24. Link S, Burda C, Nikoobakht B, El-Sayed MA. Laser-induced shape changes of colloidal gold nanorods using femtosecond and nanosecond laser pulses. J. Phys. Chem. B. 2000; 104:6152–6163.
25. Fayer M. Picosecond holographic grating generation of ultrasonic waves. IEEE Journal of Quantum Electronics. 1986; 22:1437–1452.
26. Brukh R, Mitra S. Kinetics of carbon nanotube oxidation. J. Mater. Chem. 2007; 17:619–623.
27. Zhao N, He C, Jiang Z, Li J, Li Y. Physical activation and characterization of multi-walled carbon nanotubes catalytically synthesized from methane. Materials Letters. 2007; 61:681–685.
28. Huang X, El-Sayed IH, Qian W, El-Sayed MA. Cancer cell imaging and photothermal therapy in the near-infrared region by using gold nanorods. J Am Chem Soc. 2006; 128:2115–2120. [PubMed: 16464114]
29. Zarnitsyn VG, Prausnitz MR. Physical parameters influencing optimization of ultrasound-mediated DNA transfection. Ultrasound Med. Biol. 2004; 30:527–538. [PubMed: 15121255]
30. Guzman HR, Nguyen DX, Khan S, Prausnitz MR. Ultrasound-mediated disruption of cell membranes I: Quantification of molecular uptake and cell viability. J. Acoust. Soc. Am. 2001; 110:588–596. [PubMed: 11508983]
31. Schlicher RK. Mechanism of intracellular delivery by acoustic cavitation. Ultrasound Med Biol. 2006; 32:915–924. [PubMed: 16785013]

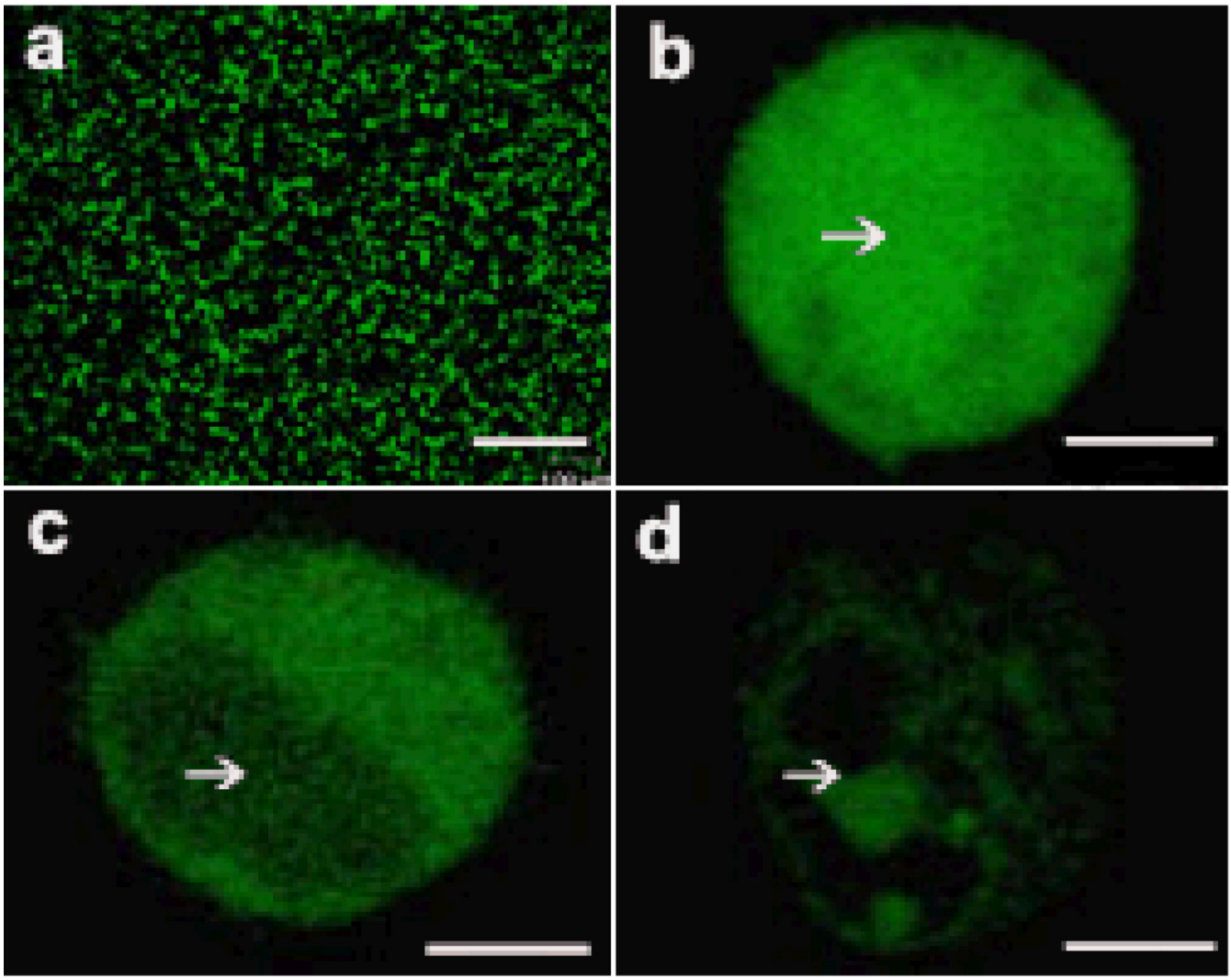


**Figure 1.**

Intracellular uptake in cells exposed to femtosecond laser irradiation in presence of CB. Confocal micrographs show irradiated DU145 cells with uptake of calcein (a,b), FITC-BSA (c) and YOYO1-DNA (d). A large population of cells exhibited uptake of calcein when viewed at 10X magnification (a). Under 40X magnification, calcein (b) is seen at high concentration throughout the cell, including the nucleus (indicated by white arrow), while BSA (c) and DNA (d) were largely excluded from the nucleus. Samples were irradiated at 5mJ/cm$^2$ for 10 min in 30μg/ml CB. Scale bars are 100μm (a) and 5μm (b–d).

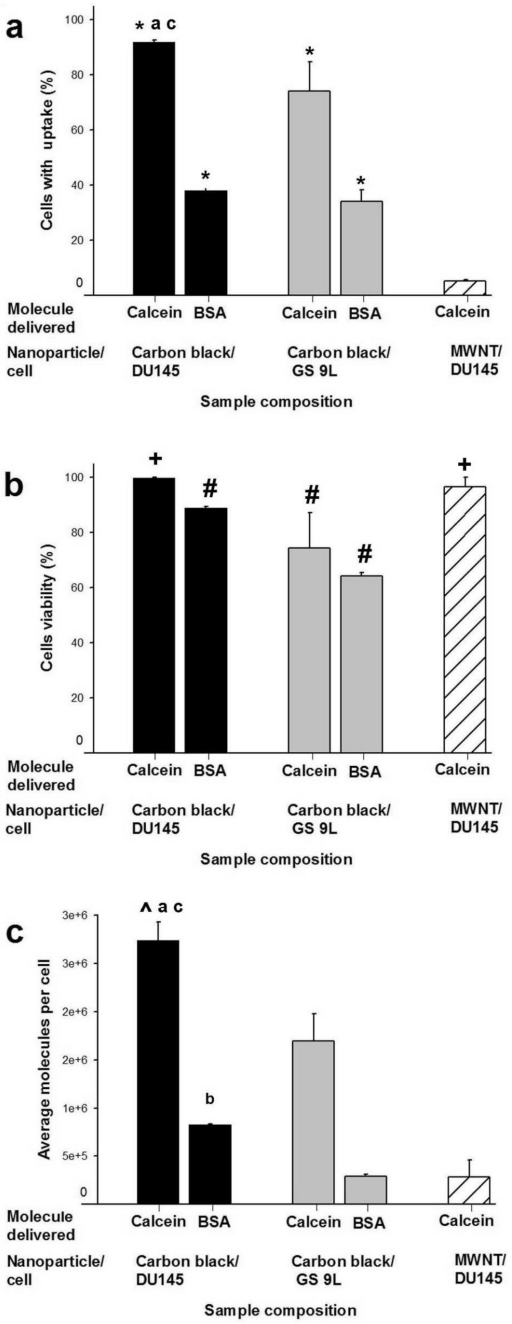


**Figure 2.**

Effect of CB nanoparticle and cell type on uptake and viability. CB were used to deliver calcein and BSA proteins into DU145 cells (■) and GS-9L cells (□). MWNT were used to deliver calcein into DU145 cells (▨). Graphs show percentage of cells with intracellular uptake (a), cell viability (b), and average number of molecules delivered per cell (c), as a function of nanoparticle and cell type. CB and MWNT were added at final concentrations of 30μg/ml. Samples were irradiated at 5mJ/cm$^2$ for 10 min. Data show average ($n$=3) ± SEM. *$p<0.05$ for cells with uptake of model drug compared to non-irradiated control (data not

shown), #$p<0.05$ for cell viability compared to non-irradiated control, +$p>0.05$ for cell viability compared to non-irradiated control, ^$p<0.05$ for calcein molecule/cell compared to non-irradiated control, $^{a}p>0.05$ for DU145 cells compared to GS-9L cells, $^{b}p<0.05$ for DU145 cells compared to GS-9L, $^{c}p<0.05$ for CB compared to MWNT. See S.I. Section 1.6 for statistical methods.

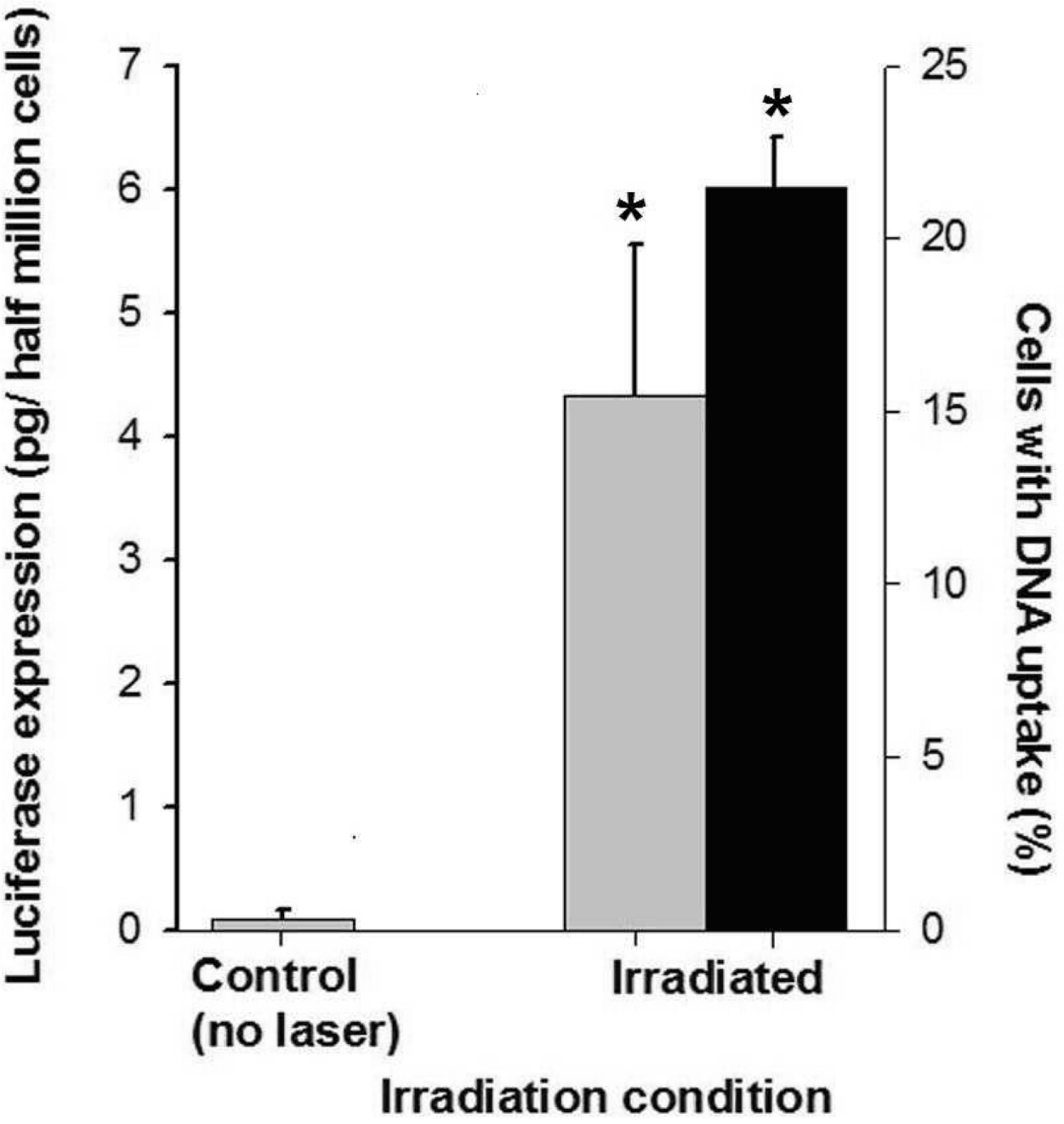


**Figure 3.**

Uptake and expression of plasmid DNA. The graph shows intracellular uptake (■) and transfection (□) of luciferase plasmid DNA in DU145 cells. Uptake of YOYO1-labeled plasmid DNA was assayed < 2h after irradiation to assess intracellular delivery of DNA molecules. Luciferase expression was measured 48h after irradiation to assess expression of the luciferase protein encoded in the DNA. Each sample had $5\times10^5$ cells and 30μg/ml CB. Irradiation was carried out at 5mJ/cm$^2$ for 10 min. Non-irradiated controls were identical to

irradiated samples, except no laser irradiation was applied. Data show average ($n$=3) ± SEM. *p<0.05 for treated cells compared to non-irradiated negative control.

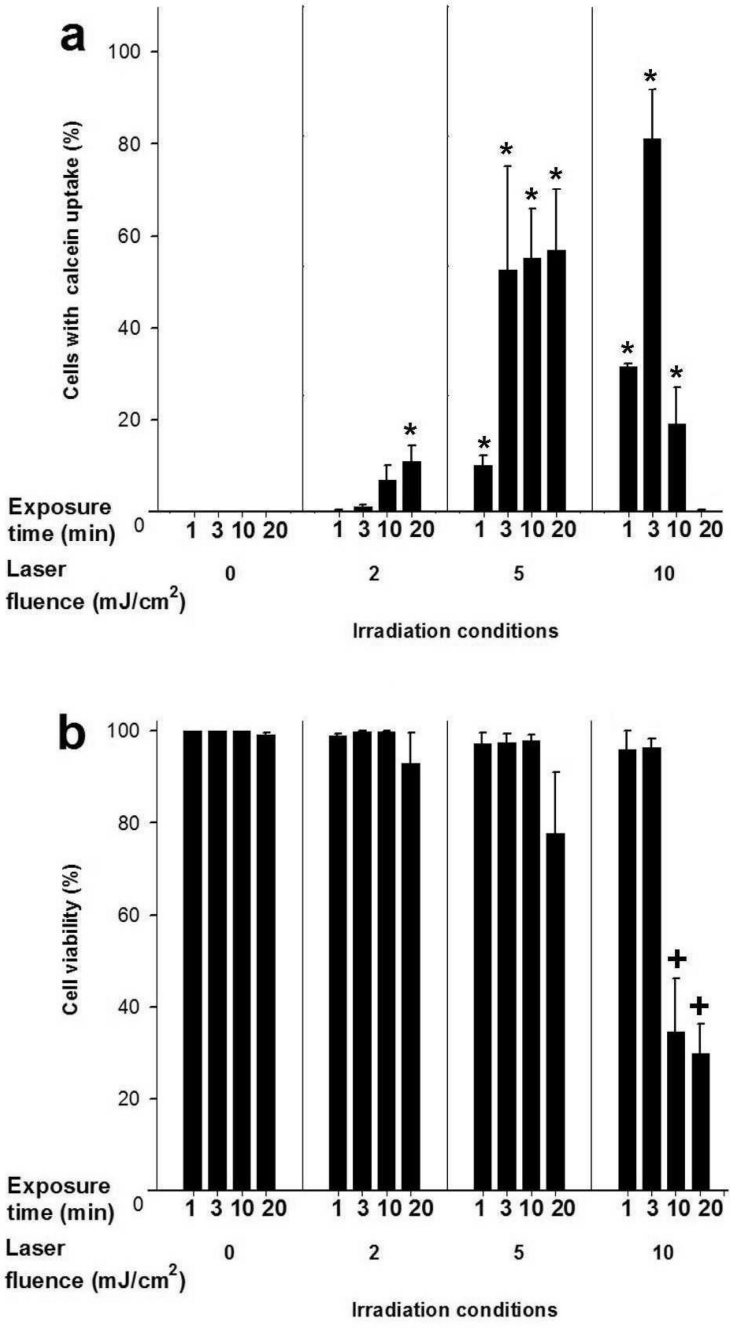


**Figure 4.**

Effect of laser fluence and exposure time on intracellular calcein uptake and cell viability in DU145 cells. Samples were irradiated in 30μg/ml CB. Data show average (*n*=3) ± SEM. *p<0.05 for cells with uptake compared to non-irradiated control at the same exposure time, $^{+}$p<0.05 for cell viability compared to non-irradiated control at the same exposure time.

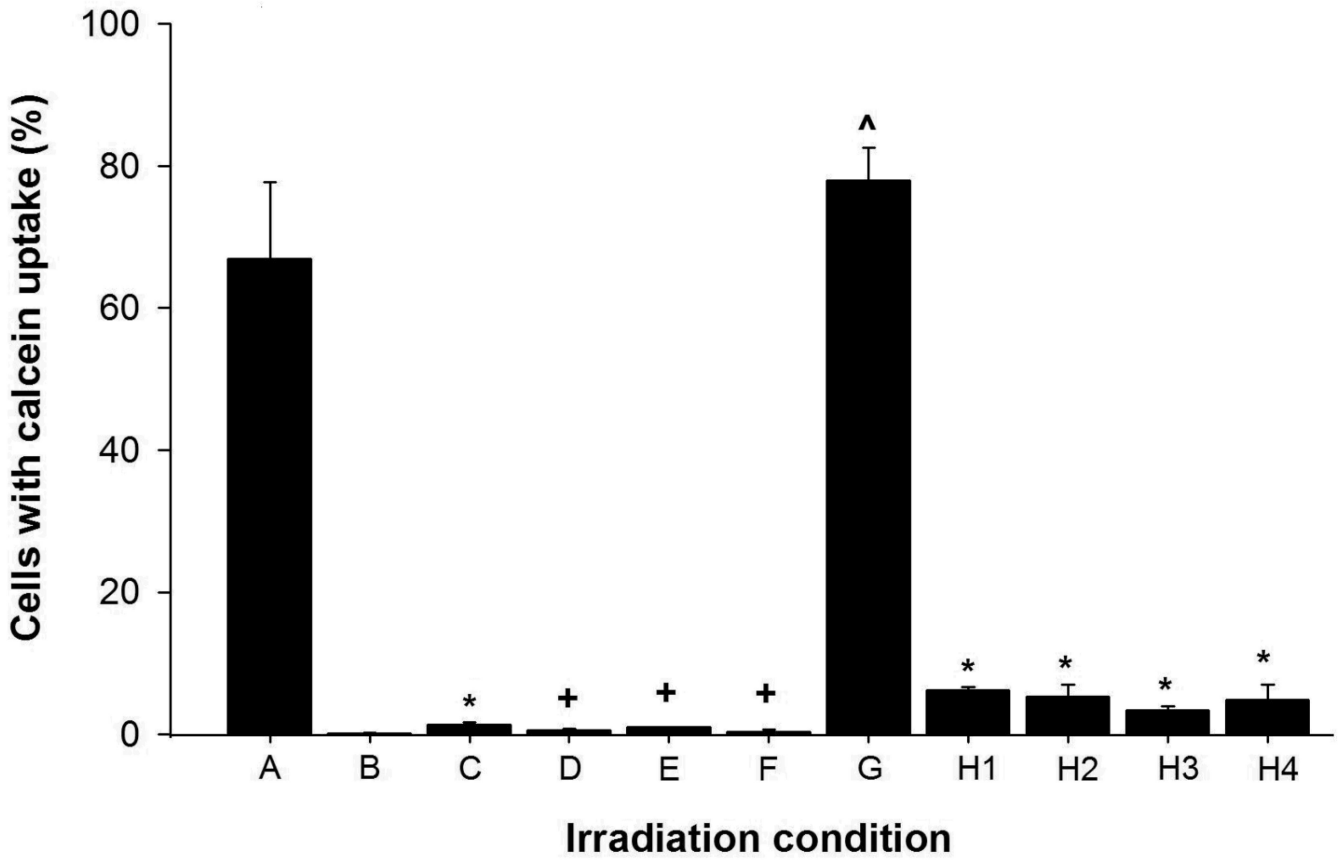


**Figure 5.**

Effect of irradiation conditions on intracellular uptake of calcein in DU145 cells. Standard conditions for this experiment were irradiation at 5mJ/cm$^2$for 10 min with 30μg/ml CB and 10μM calcein. Deviations from standard conditions are as follows. (A) Positive control (standard conditions). (B) Non-irradiated negative control (standard conditions without irradiation). (C) Irradiation without CB. (D) Irradiation with gold nanorods instead of CB. (E) Cells added <1s after irradiation of cell-free solution containing CB and calcein. (F) Irradiation in media with five-fold higher viscosity. (G) Irradiation of cells pre-treated in $K^+$-depleted media to block endocytic processes. (H) Calcein added < 1s (H1), 30s (H2), 60s (H3) and 120s (H4) after irradiation for 3 min. Data are expressed as the percentage of cells with calcein uptake among all irradiated cells, except for (G), in which data are expressed as the percentage of viable cells with calcein. This correction was made in (G) because the $K^+$-depletion pre-treatment to suppress endocytosis killed ~20% of cells. Data show average ($n$=3) ± SEM. *p<0.05 for cells with uptake compared to condition A, $^+$p>0.05 for cells with uptake compared to condition B, ^p>0.05 for cells with uptake compared to condition A.